JOURNAL OF MATERIALS SCIENCE 16 (1981) 1689–1699

Effect of hydrostatic pressure on the yield and fracture of polyethylene in torsion

R. W. TRUSS, R. A. DUCKETT, I. M. WARD
Department of Physics, The University of Leeds, Leeds, UK

Yield and fracture of polyethylene have been studied in torsion tests under superposed hydrostatic pressures. Two ductile-to-brittle transitions have been observed. At high strain rates and pressures, a conventional ductile-to-brittle transition was found with increasing strain rate and pressure. A second ductile-to-brittle transition was observed at low strain rates with decreasing strain rate. The yield stress showed a region of low, relatively constant, rate dependence at low strain rates, high temperatures and low pressures and a second region of higher strain-rate dependence at high strain rates and pressures. In contrast, the fracture stress was found throughout to have a relatively constant strain-rate dependence of intermediate value between those obtained for the yield stress. These features confirmed that failure can be considered as competition between yield and fracture processes. The fracture stress became lower than the yield stress at both high and low strain rates where brittle fracture was observed, with fully ductile behaviour resulting in intermediate conditions where the fracture stress exceeded the yield stress. The pressure, strain rate and temperature dependence of the yield stress was well described by two Eyring processes acting in parallel, both processes being pressure dependent.

1. Introduction

It is known that some polyethylene materials subjected to loads well below their normal yield stress can fail in an unexpectedly brittle fashion when in contact with certain environments such as detergents. This subject is reviewed by Howard [1]. Predictions of the behaviour of polyethylene components under low loads in various environments have been hampered by lack of data owing to the excessively long times for brittle failure to occur in low-load laboratory tests. This present research programme was undertaken to obtain information on brittle failure of polyethylene in short-term tests.

In previous work, Rabinowitz *et al.* [2] showed that the shear yield stress of polymethylmethacrylate (PMMA) was increased by applied hydrostatic pressure to a greater extent than its fracture stress, so that PMMA which was normally ductile at atmospheric pressure could be made to respond in a brittle fashion when tested under hydrostatic pressures greater than $\sim 320\,MN\,m^{-2}$. This work also showed that the shear yield stress of polyethylene was increased by hydrostatic pressure. This present work was initiated to investigate more fully the effects of hydrostatic pressure on the shear yield behaviour of polyethylene and to discover whether the application of sufficiently high hydrostatic pressure could induce brittle failure in polyethylene in a similar fashion to PMMA.

2. Equipment and materials

The high-pressure torsion apparatus employed in these experiments was originally described by Rabinowitz *et al.* [2] with modifications made by Joseph and Duckett [3]. It allowed torque–twist curves to be obtained at constant twist rates from $\sim 10^{-5}$ to $5 \times 10^{-1}\,rad\,sec^{-1}$ at temperatures from 20 to $\sim 80^{\circ}C$. Hydrostatic pressures of up to $500\,MN\,m^{-2}$ could be applied to the test sample.

The testing procedure produced data in the form of torque–twist curves. Shear stress–strain curves were calculated from the torque–twist curves using an analysis due to Nadai [4] in which the shear stress, τ, at the surface of a cylinder of

0022–2461/81/061689–11$03.10/0

TABLE I Characterization of polyethylene grades used in these experiments

Polyethylene grade	$\bar{M}_W$	$\bar{M}_N$	Density	Branch content
Rigidex 50	101 450	6 180	0.972	linear
Rigidex 002-40	134 000	20 800	0.945	~ 4 butyl groups/10^3 C atoms
Rigidex 006-60	135 000	25 500	0.963	linear

radius, b, can be calculated from the measured torque, M, by

$$\tau = \frac{1}{2\pi}\left[\frac{3M}{b^3} + \gamma\frac{d}{d\gamma}\left(\frac{M}{b^3}\right)\right],$$

where γ, the shear strain on the surface of the cylinder is given by

$$\gamma = b\phi,$$

where ϕ is the twist per unit length of the cylinder. No attempt was made to compensate for the strain-rate dependence of the shear stress.

Three grades of polyethylene were tested and these are listed in Table I. These materials were commercially available polyethylene manufactured by B.P. Chemicals Ltd. Rigidex 50 and Rigidex 006-60 were high-density homopolymers while Rigidex 002-40 was a medium-density co-polymer. The Rigidex 002-40 material was a gas-pipe grade of polyethylene and as such contained a yellow pigment for identification purposes. The majority of the experiments were conducted on Rigidex 50 and Rigidex 002-40 samples. A few fracture results on Rigidex 006-60 are included for comparison purposes.

The samples were in the form of 8 and 10 mm diameter solid cylinders with square-shouldered ends to permit the application of a torque to the cylinder. Specimens of Rigidex 50 and Rigidex 006-60 were injection-moulded and had a gauge length of 25.4 mm while the samples of Rigidex 002-40 were machined from compression-moulded blocks and had a gauge length of 31.75 mm.

The fracture tests on these materials required the specimens to be notched and tested in an agressive environment. Notching of the samples was achieved by pressing a new razor blade into the surface of the sample at an angle of 45° to the axis of the sample. A special jig was constructed to fit on the compression stage of an Instron testing machine so that the razor blade could be pressed into the specimen to a given load ensuring reasonably constant notch depth. The average notch depth for the Rigidex 50 samples was 0.63 mm (± 5%). The notches in the Rigidex 002-40 samples were slightly deeper owing to the slightly different resistance of this material to the penetration of a razor blade.

To facilitate a controlled environment, the specimens were enclosed in thin rubber sheaths into which the desired environment could be introduced. In the majority of these experiments, the environment was a 10 vol % solution of Igepal 730 in distilled water. Igepal is a nonylphenoxy-poly(ethyleneoxy)ethanol and is a non-ionic surfactant. The rubber sheath was found to contribute a negligible amount to the measured torque on the sample.

3. Results

3.1. Rigidex 50

3.1.1. General features

The effect of increasing pressure on the stress–strain behaviour of Rigidex 50 samples in torsion tests at 20° C and at a constant strain rate of $9.4 \times 10^{-4}\,\text{sec}^{-1}$ is shown in Fig. 1. No attempt was made to protect the samples in Fig. 1 from the pressure-transmitting fluid, castor oil. It can be seen that there was an increase in the initial modulus of the material with increasing pressure and that, at all pressures up to $400\,\text{MN m}^{-2}$, this material behaved in a ductile fashion and did not fail up to strains of ~ 30% which was the limiting strain used in these experiments.

In general, no maximum was observed in the stress–strain curves for polyethylene which would correspond to a yield point. Thus a 2% offset or proof stress was taken as an indication of the yield stress. Fig. 2 shows the shear yield stress, τ_y, plotted against the applied hydrostatic pressure for Rigidex 50 tested at 20° C and a strain rate of $9.4 \times 10^{-4}\,\text{sec}^{-1}$ and also at 50°C and a strain rate of $2.6 \times 10^{-5}\,\text{sec}^{-1}$. (The error bars on the data points in Fig. 2 are ± 5% of the average value of the yield stress obtained from several tests and represent a reasonable estimate of the scatter in the experimental data.) The yield stress increased approximately linearly with pressure but it can be seen from the figure that the slope of 0.035 at 50°C and a strain rate of $2.6 \times 10^{-5}\,\text{sec}^{-1}$ was sig-

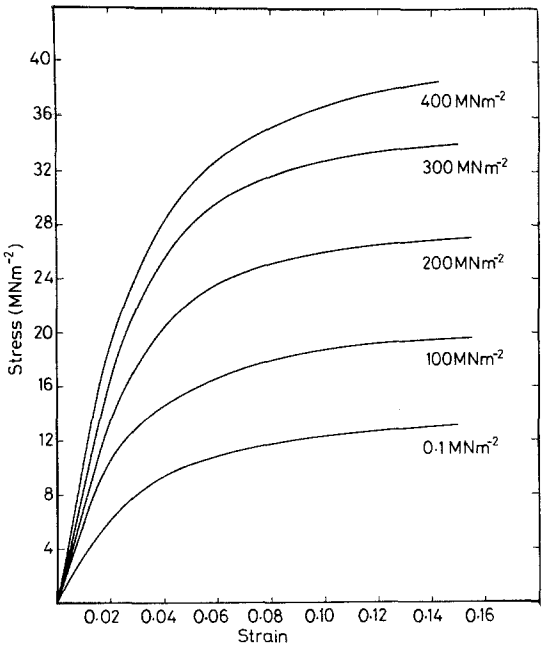

Figure 1 Shear stress–strain curves for Rigidex 50 tested in torsion at 20°C and a strain rate of 9.4×10^{-4} sec^{-1} and at various pressures.

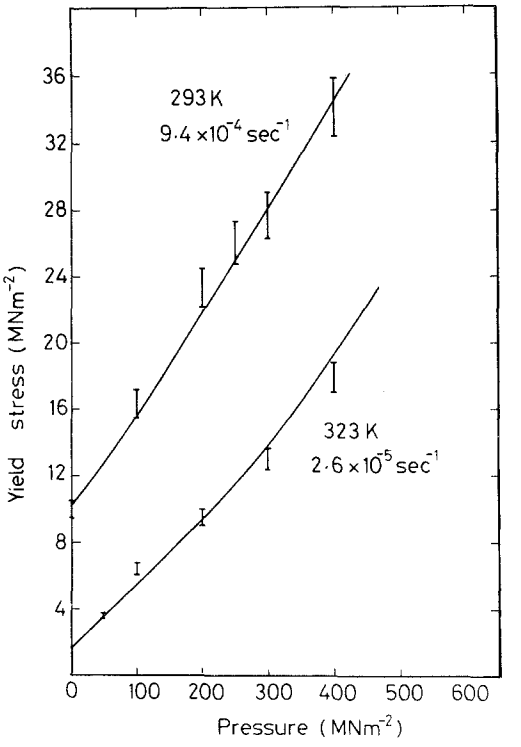

Figure 2 Shear yield stress as a function of pressure for Rigidex 50 tested at 293 K and a strain rate of 9.4×10^{-4} sec^{-1} and at 323 K at a strain rate of 2.6×10^{-5} sec^{-1}. Curves as calculated from the Eyring theory.

nificantly less than the slope of 0.063 at 20° C and a strain rate of 9.4×10^{-4} sec^{-1}. The lines through the data points in Fig. 2 have slight curvatures, and have been calculated from an Eyring rate theory which will be discussed in a subsequent section.

Fig. 3 shows the yield stress as a function of strain rate for a series of temperatures and pressures. At a pressure of 250 MN m^{-2} at 293 K, the yield stress varied approximately linearly with log (strain rate). However, at higher temperatures or lower pressures, the plot of τ_y/T against $\log \dot{\gamma}$ showed distinct curvature, the strain-rate dependence of the yield stress increasing with increasing strain rate. At atmospheric pressure and 293 K at strain rates below $\sim 3 \times 10^{-4}$ sec^{-1} and at 50 MN m^{-2} pressure at 323 K below a strain rate of $\sim 6 \times 10^{-4}$ sec^{-1}, the plots again appeared to be linear. The data in Fig. 3 are plotted as τ_y/T against $\log \dot{\gamma}$ suggested by the Eyring rate theory for yield and lines drawn through the data points in Fig. 3 are theoretical lines calculated from this theory. This will be discussed later.

Fig. 4 shows the temperature dependence of the yield stress of Rigidex 50 tested at a pressure of 250 MN m^{-2} at a strain rate of 9.4×10^{-4} sec^{-1}. The yield stress decreased approximately linearly with increasing temperature from 20 to 70° C. Again the line through the data was calculated from the Eyring theory.

3.1.2. Notched samples

The effects of pressure on the shear stress–strain curves of notched samples of Rigidex 50 tested in Igepal solution at 20° C and a strain rate of 9.4×10^{-4} sec^{-1} are shown in Fig. 5. At atmospheric pressure, notched samples of Rigidex 50 tested in Igepal solution remained ductile and the specimens did not fracture up to 30% strain. With the application of hydrostatic pressure of 100 MN m^{-2}, Rigidex 50 still showed extensive ductility but the specimens fractured at strains less than 30%. With increasing hydrostatic pressure, the strain to fracture decreased until at pressures above ~ 250 MN m^{-2}, the samples fractured before attaining a 2% offset proof stress, that is, the material behaved in an essentially brittle fashion. The stress–strain curves of those notched samples which did not fracture were not significantly affected by the presence of the notch or the Igepal solution. The stress–strain curves for the notched samples which did fracture were also the same as the normal stress–strain curves for unnotched samples up to the point where the crack growth occurred from the notch. At this point, the stress–strain curve for the notched samples decreased

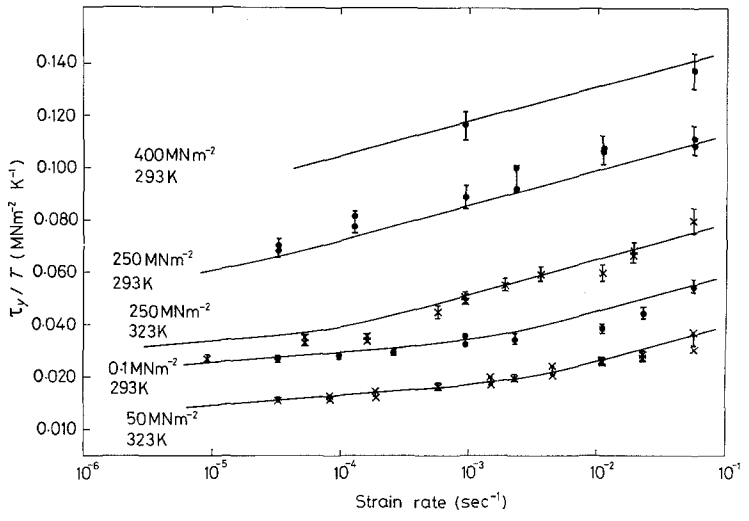

Figure 3 Shear yield stress of Rigidex 50 as a function of strain rate, temperature and pressure. Lines calculated from the Eyring theory.

whereas the normal stress–strain curve for an unnotched sample continued to increase. This maximum in the stress–strain curve for the notched samples was taken as the fracture stress.

Fig. 6 shows the fracture stress plotted as a function of applied hydrostatic pressure. Although there was a degree of scatter in the fracture stress data, it can be seen that the fracture stress increased approximately linearly with pressure and that the pressure dependence of the fracture stress, approximately 0.02, was considerably less than that found for the yield stress, 0.063. Fig. 7 shows the strain-rate dependence of the fracture stress, τ_F, at different temperatures and pressures. They are plotted in the Eyring fashion of τ_F/T against $\log \dot{\gamma}$ so that they can be directly compared to the yield data. At a pressure of 250 MN m^{-2} at 293 or 323 K, and at a pressure of 400 MN m^{-2} at 293 K, the fracture stress appeared to vary linearly with log (strain rate) and, moreover, the strain-rate dependence of the fracture stress was approximately independent of temperature and

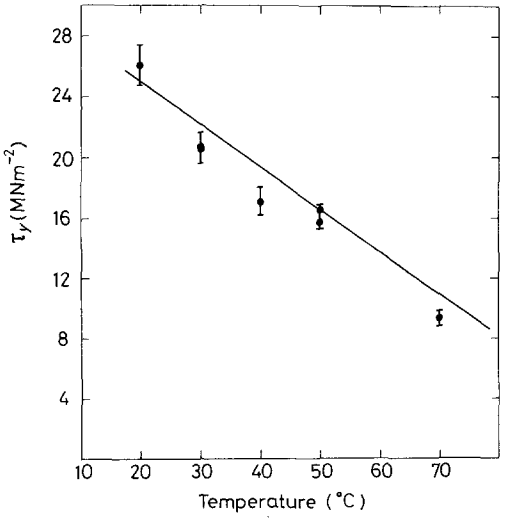

Figure 4 Shear yield stress of Rigidex 50 as a function of temperature at 250 MN m^{-2} pressure and a strain rate of 9.4 × 10^{-4} sec^{-1}.

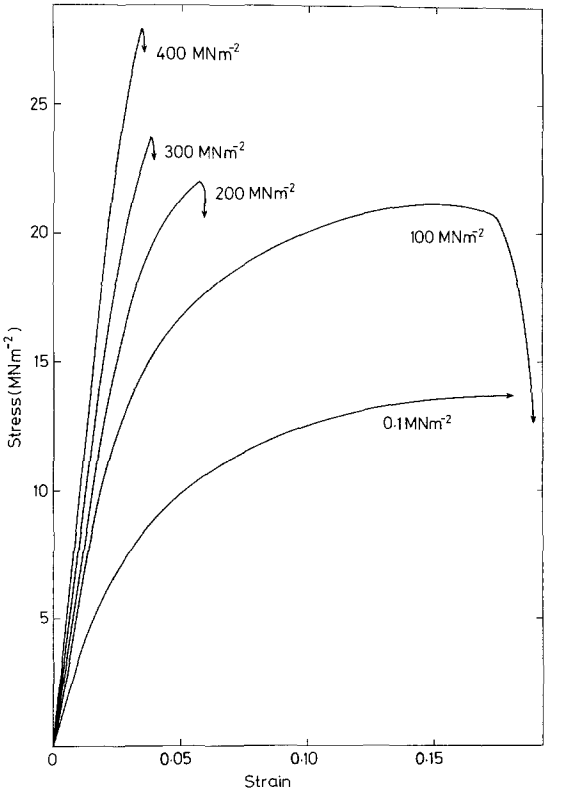

Figure 5 Stress–strain curves of notched samples of Rigidex 50 tested in Igepal solution at 293 K and a strain rate of 9.4 × 10^{-4} sec^{-1}.

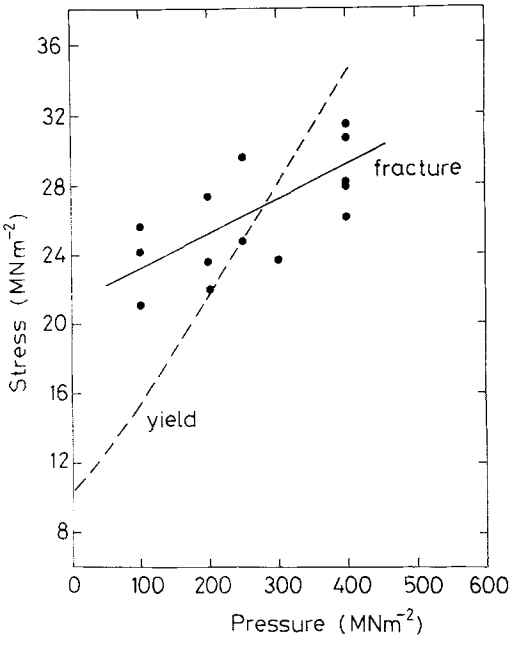

Figure 6 Fracture stress as a function of pressure for notched samples of Rigidex 50 tested in Igepal solution at 293 K and a strain rate of 9.4×10^{-4} sec^{-1}.

pressure. At high strain rates, high pressures and low temperatures, the strain-rate dependence of the yield stress was greater than that of the fracture stress; at low strain rates, high temperatures and low pressures, the strain-rate dependence of the yield stress was greater than that for yield.

When Rigidex 50 was tested at a pressure of 400 MN m^{-2} at 293 K, it failed in a brittle fashion over the whole range of strain rates. This implies that the fracture stress was lower than the yield stress at all strain rates used at this pressure. Notched samples of Rigidex 50 tested at the lower pressure of 250 MN m^{-2} at 293 K failed after considerable ductility at a strain rate of 3×10^{-5} sec^{-1}. With increasing strain rate at this temperature and pressure, the fracture strain decreased until at strain rates greater than approximately 10^{-2} sec^{-1}, the material failed before attaining its yield point. This is the approximate strain rate at which the yield stress curve and the fracture stress curve intersect in Fig. 7 for this temperature and pressure. At a pressure of 250 MN m^{-2} at 323 K, Rigidex 50 fractured at strain rates greater than 5×10^{-4} sec^{-1} but only after considerable ductility. It is anticipated that an intersection of the yield stress and fracture stress lines under these conditions would occur at a strain rate $> 10^{-1}$ sec^{-1}. Thus the intersections of the yield stress and the fracture stress lines in Fig. 7 reflected the onset of brittle failure in the material, samples failing before attaining their yield stress at strain rates greater than those at which the yield stress lines and the fracture stress lines intersect. At strain rates slightly less than those at which the yield stress lines and fracture stress lines intersect, the material still failed but only after significant ductility.

The strain-rate dependence of the yield stress decreased with decreasing strain rate (Fig. 3). It would be expected that a second set of intersections between the yield stress and the fracture stress lines could occur at low strain rates. A linear extrapolation of the data suggests that the intersection would occur at a strain rate of 10^{-9} sec^{-1} at 293 K and a pressure of 250 MN m^{-2} and at a strain rate of 3.5×10^{-7} sec^{-1} at 323 K and a pressure of 250 MN m^{-2}. This would indicate a ductile-to-brittle transition with decreasing strain rate but unfortunately, the strain rates at which these transitions would occur for Rigidex 50 were lower than those available on the present equipment.

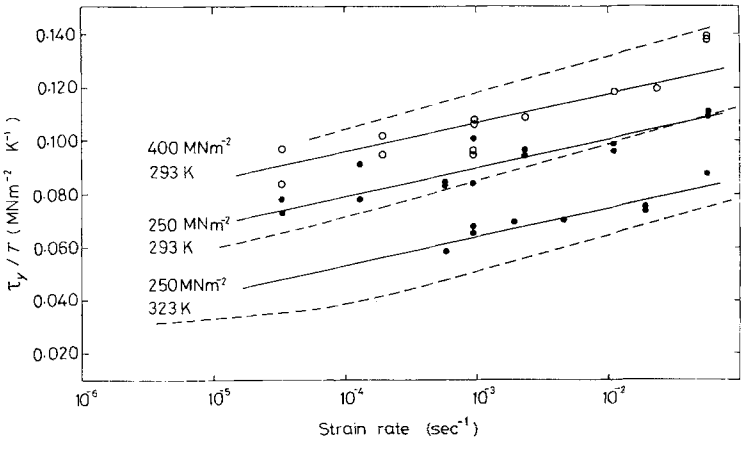

Figure 7 Fracture stress of notched samples of Rigidex 50 tested in Igepal solution as a function of strain rate, temperature and pressure. (- - - - - - yield lines from Fig. 3.)

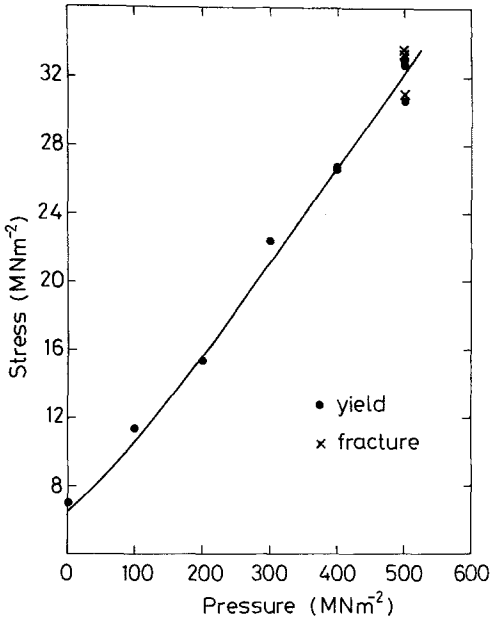

Figure 8 Shear yield stress (•) and fracture stress (X) of Rigidex 002-40 as a function of pressure. Test conditions: 293 K, strain rate 9.4×10^{-4} sec^{-1}.

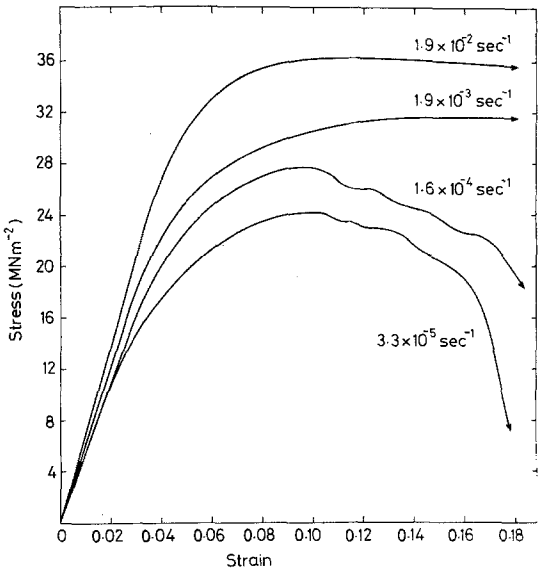

Figure 9 Stress–strain curves for notched samples of Rigidex 002-40 tested in Igepal solution at 400 MN m^{-2} pressure at 293 K and at various strain rates.

3.2. Rigidex 002-40

The effects of pressure on the yield and fracture behaviour of Rigidex 002-40 polyethylene tested at 293 K and at a strain rate of 9.6×10^{-4} sec^{-1} are summarized in Fig. 8. This material behaved in a similar fashion to Rigidex 50 except that the Rigidex 002-40 material remained ductile to the much higher pressure of 400 MN m^{-2}. Only at a pressure of 500 MN m^{-2} did this material fracture at strains below 30% and then considerable ductility was still observed before failure. The magnitude of the yield stress for Rigidex 002-40 at a given pressure was less than that of Rigidex 50 but the pressure dependence of the yield stress did not appear to be significantly different from that of Rigidex 50.

Fig. 9 shows the effect of strain rate on the shear stress–strain curves of notched samples of the Rigidex 002-40 material tested in Igepal solution at 20° C and at a pressure of 400 MN m^{-2}. The material showed the expected decrease in the initial modulus and the yield stress with decreasing strain rate. What is more significant, however, was that at strain rates $\geqslant 1.9 \times 10^{-3}$ sec^{-1}, the samples were ductile while at lower strain rates the specimens fractured at nominal strains of less than 10%. This information is shown in Fig. 10 which is an Eyring-type plot of the yield and fracture data for the Rigidex 002-40 material at 400 MN m^{-2} pressure and 293 K. At high strain rates, the slope of the Eyring plot for Rigidex 002-40 material was similar to that obtained for Rigidex 50 at 293 K and 400 MN m^{-2} pressure. At lower strain rates, the strain-rate dependence of the yield stress for Rigidex 002-40 material tended to decrease in a similar manner to Rigidex 50 at lower pressures and higher temperatures (Fig. 3). It was in this region that the Rigidex 002-40 material began to fail. The line through the fracture stress data in Fig. 10 has been drawn with the same slope as that obtained for fracture in Rigidex 50 (Fig. 7) since the actual slope could not be determined accurately from the three data points.

4. Discussion

4.1. Ductile-to-brittle and brittle-to-ductile transitions

Brittle failure and yield can be considered as competing processes. A material under given test conditions will yield or fail in a brittle fashion depending on which of these two modes of deformation occurs at the lower stress at the given test conditions. It has been shown in Fig. 6 that the pressure dependence of the fracture stress of Rigidex 50 polyethylene was significantly lower than the pressure dependence of its yield stress. Thus with the application of sufficiently high hydrostatic pressure, the yield stress of this material was made higher than its fracture stress

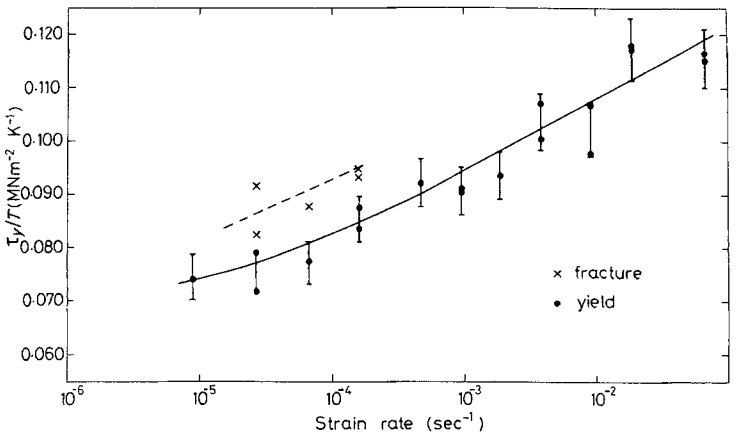

Figure 10 Yield stress (———) and fracture stress (– – – –) as a function of strain rate for notched samples of Rigidex 002-40 tested in Igepal solution at a pressure of 400 MN m^{-2} at 293 K.

and the behaviour of the material underwent a ductile-to-brittle transition. Similarly, the strain-rate dependence of the fracture stress of Rigidex 50 at high strain rates, high pressures or low temperatures was less than the strain-rate dependence of the yield stress under these test conditions (Fig. 6) and the material underwent a ductile-to-brittle transition with increasing strain rate as the yield stress exceeded the fracture stress. This was similar behaviour to other polymers such as PMMA [2] and polycarbonate [5] which show a ductile-to-brittle transition with increasing pressure or decreasing temperature, and parallels the work of Mears *et al.* [6] who found a decrease in the strain-to-failure with increasing pressure for polyethylene tested in tension in a pressure medium of kerosene–oil mixture. Trent *et al.* [7] observed a similar reduction in the failure strain with increasing pressure for polyethylene tested in tension in silicone oil.

The decrease in the strain-rate dependence of the yield stress with decreasing strain rate suggested that the fracture stress could again become lower than the yield stress at very low strain rates. For Rigidex 50, this condition would have been reached at strain rates well below those available on the present equipment. However, evidence for this second ductile-to-brittle transition with decreasing strain rate was observed in the Rigidex 002-40 material. Although extensive yield and fracture data were not obtained for this material, the yield stress and the fracture stress curves plotted as functions of log (strain rate) at 293 K and a pressure of 400 MN m^{-2} could be extrapolated at high strain rates to intersect at a strain rate $> 10^{-1}$ sec^{-1} and again extrapolated to low strain rates to intersect at a strain rate between 10^{-7} and 10^{-6} sec^{-1}. The intersection at high strain rate would correspond to the ductile-to-brittle transition already discussed for Rigidex 50. As with Rigidex 50, this ductile-to-brittle transition was also observed in Rigidex 002-40 with increasing pressure (Fig. 8). At strain rates just lower than those required to cause conventional high strain-rate brittle fractures in Rigidex 50, a region of strain rate was observed in which samples fractured after a degree of ductility. It would be expected that a similar region of strain rate in which failure occurred after a degree of ductility would also be observed with decreasing strain rate as the projected intersection of the yield stress and the fracture stress lines at low strain rates was approached. This phenomenon was observed in the Rigidex 002-40 material, confirming the possibility of a ductile-to-brittle transition with decreasing strain rate.

In constant strain-rate tests, a ductile-to-brittle transition in polyethylene with decreasing strain rate has not previously been observed. It should be noted that brittle failure of polyethylene in these experiments could only be induced by notching the samples and subjecting them to an aggressive environment under pressure. The need for the environment suggests that the brittle-to-ductile transition with decreasing strain rate found for polyethylene in this work may be related to the environmental stress cracking observed in polyethylenes subjected to low loads for long times [1], the effect of hydrostatic pressure being to reduce the time scale at which the phenomenon is observed. Short-term tests conducted at high pressure may thus prove a useful technique for the study of long-term failure of polyethylene under low loads.

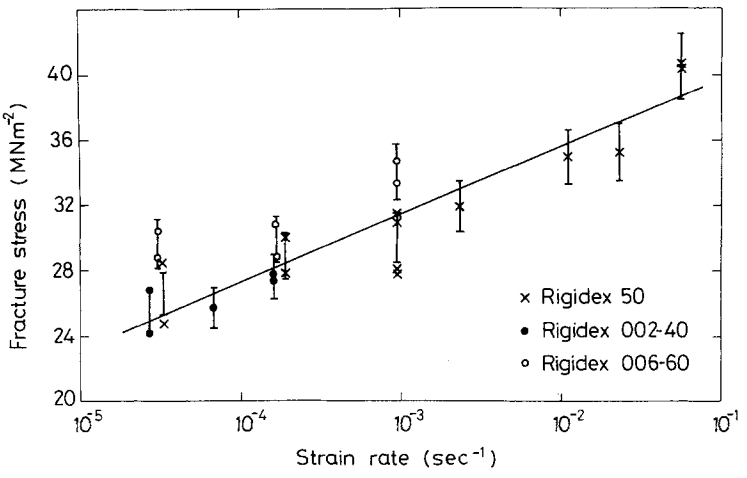

Figure 11 Fracture stress as a fucntion of strain rate for Rigidex 50 (×) Rigidex 002-40 (•) and Rigidex 006-60 (○). Temperature = 20° C, pressure 400 MN m^{-2}.

It is interesting to note that the fracture stress of Rigidex 50 and Rigidex 002-40 tested under the same conditions were very similar even though these two materials were quite different polyethylenes, Rigidex 50 being a high-density homopolymer and Rigidex 002-40 a medium-density co-polymer. Several tests were also conducted on a third grade of polyethylene, Rigidex 006-60, and it was found that its fracture stress was also of a similar magnitude to Rigidex 50 and Rigidex 002-40. This can be seen in Fig. 11 in which the fracture stresses for the three grades of polyethylene tested at a pressure of 400 MN m^{-2} at 20° C are plotted against log (strain rate). The small differences in the fracture stresses of Rigidex 50, Rigidex 002-40 and Rigidex 006-60 may not be significant since they may have resulted from slight differences in the notch depths among the materials. The notch was produced by pressing a razor blade into the samples under the same load for each material and since each grade of polyethylene had a slightly different resistance to the penetration of a razor blade, this notching procedure produced a slight variation in the notch depth with different materials. Despite this slight uncertainty, the results shown in Fig. 11 do suggest that the fracture stress did not vary greatly between different grades of polyethylene and, consequently, the difference in behaviour of different grades of polyethylene resulted primarily from variations in their yield behaviour. The Rigidex 002-40 had a lower yield stress than the homopolymer grades tested here and resulted in it failing in a ductile manner over a wider range of test conditions than that seen for the homopolymers. This greater resistance to brittle fracture resulting from the lower yield stress is the essential reason why the co-polymer material has found utilization as a gas-pipe grade polyethylene.

One further point is worthy of note in relation to the fracture behaviour. The environment used in the fracture experiments was a 10 vol % solution of Igepal 730 in distilled water. Igepal was chosen as it is the recommended environment for standard tests on the susceptibility of a polyethylene material to environmental stress cracking [8]. It is interesting to note that in the course of this work, distilled water was found to be only slightly less aggressive than Igepal solution as an environmental stress cracking agent. For example, samples of Rigidex 50 tested in Igepal solution at 293 K and a strain rate of 9.4×10^{-4} sec^{-1} failed at strains of less than 30% at pressures of 100 MN m^{-2} and above. With distilled water as the environment, samples of Rigidex 50 tested under the same conditions of strain rate and temperature were ductile at a pressure of 100 MN m^{-2} but failed at pressures of 200 MN m^{-2} and above. Although the test conditions of high pressure used here were severe, this result does suggest that a water environment for polyethylene may not be as benign as is generally accepted.

4.2. Yield behaviour

In view of the importance of the yield behaviour to the response of a grade of polyethylene under stress, it would seem advantageous to be able to describe yield in a more quantitative fashion. Although there is some doubt as to its physical significance, a theory due to Eyring [9] has been found to describe the yield behaviour of many glassy polymers to a reasonable accuracy. It is used here as it provides a relatively simple model

to describe the present yield data. Polymer flow is considered as an activated process, the strain rate, $\dot{\gamma}$, at a stress, τ, being given by

$$\dot{\gamma} = 2A \sinh\left(\frac{\tau v}{kT}\right) \exp\left(-\frac{\Delta H}{kT}\right), \quad (1)$$

where ΔH is the activation energy, T is the absolute temperature, v is a constant with the units of volume generally called the stress activation volume, A is a constant and k is Boltzmann's constant. At high stresses ($\tau v \gg kT$) back reaction over the energy barrier can be neglected, and the equation can be simplified as follows

$$\dot{\gamma} = A \exp\left\{-\left(\frac{\Delta H - \tau v}{kT}\right)\right\}. \quad (2)$$

Ward [10] has previously suggested that the Eyring equation may be very simply modified to include the effect of hydrostatic pressure on the yield stress. He gave a modified form of the high stress Eyring Equation 1 as

$$\dot{\gamma} = A \exp\left\{-\frac{(\Delta H - \tau v + p\Omega)}{kT}\right\}, \quad (3)$$

where p is the hydrostatic pressure and Ω is a constant, again with units of volume, called the pressure activation volume. Equation 3 results in a shear yield stress which increases linearly with pressure according to $\tau_y = \tau_0(\gamma, T) + \alpha p$ where $\alpha = \Omega/v$. Hydrostatic pressure increases the energy barrier to be overcome by the moving elements causing flow, and results in an addition to the activation energy in Equation 1 since both forward and back activation of the flow elements are equally affected by the pressure.

Plots of the yield stress against log (strain rate) for some polymers show a distinct curvature [11–13] and a more complex form of the Eyring theory which invokes two flow processes is required to adequately describe this phenomenon. The stresses for the two processes are considered to be additive and the total stress is given by

$$\frac{\tau}{T} = \frac{k}{v_1} \sinh^{-1}\left[\frac{\dot{\gamma}}{2A_1} \exp\frac{(\Delta H_1 + p\Omega_1)}{kT}\right] + \frac{k}{v_2} \sinh^{-1}\left[\frac{\dot{\gamma}}{2A_2} \exp\frac{(\Delta H_2 + p\Omega_2)}{kT}\right]. \quad (4)$$

The constants are the corresponding constants in Equation 3, the subscripts referring to the first and second flow processes.

The distinct curvature in the plot of the yield stress for Rigidex 50 as a function of log (strain rate) (Fig. 3), suggests that a two-flow process Eyring model can be invoked to describe yield in this material. It is assumed here that the 2% offset or proof stress is an adequate measure of the yield stress under these conditions and further that the first flow process can be represented by the high stress approximation as in Equation 3. Thus

$$\frac{\tau_y}{T} = \frac{k}{v_1}\left[\ln\dot{\gamma} - \ln A_1 + \frac{(\Delta H_1 + p\Omega_1)}{kT}\right] + \frac{k}{v_2} \sinh^{-1}\left[\frac{\dot{\gamma}}{2A_2} \exp\left(\frac{\Delta H_2 + p\Omega_2}{kT}\right)\right], \quad (5)$$

where τ_y is the yield stress. At low strain rates, low pressures and high temperatures where the contribution of the second flow process to the total stress is negligible

$$\left[\frac{\partial\left(\frac{\tau_y}{T}\right)}{\partial \ln\dot{\gamma}}\right]_{p,T} = \frac{k}{v_1} \quad (6)$$

and

$$\left(\frac{\partial \tau_y}{\partial p}\right)_{\dot{\gamma},T} = \frac{\Omega_1}{v_1} = \alpha_1. \quad (7)$$

At high pressures, high strain rates and low temperatures, both flow processes can be approximated by the exponential form of the Eyring equation, and

$$\left[\frac{\partial\left(\frac{\tau_y}{T}\right)}{\partial \ln\dot{\gamma}}\right]_{p,T} = \frac{k}{v_1} + \frac{k}{v_2} \quad (8)$$

and

$$\left(\frac{\partial \tau_y}{\partial p}\right)_{\dot{\gamma},T} = \frac{\Omega_1}{v_1} + \frac{\Omega_2}{v_2} = \alpha_1 + \alpha_2. \quad (9)$$

The strain-rate dependence of the yield-stress data for Rigidex 50 was shown in Fig. 3, and the stress-activation volumes v_1 and v_2 calculated from the gradients using Equations 6 and 8 are listed in Table II. The measured slopes at low pressures, high temperatures and at high pressures, low temperatures of the yield stress against pressure curves in Fig. 2 were used to calculate α_1 and α_2 and, hence, using Equations 7 and 8, Ω_1 and Ω_2. The activation energies and the other constants in Equation 5 were obtained from the position and separation of the Eyring plots of τ_y/T against log (strain rate) at the different temperatures and

TABLE II Eyring parameters obtained for Rigidex 50

Parameter	Process 1	Process 2
v (Å^3)	6500	3700
Ω (Å^3)	225	105
α	0.035	0.063
ΔH (k cal mol^{-1})	58	24
A	1.1×10^{34}	1.5×10^{15}

pressures in Fig. 3 and all these parameters are listed in Table II. These parameters were used with Equation 5 to generate the curves through the data points in Figs 2 to 4.

It can be seen that the measured dependence of the yield stress on temperature, strain rate and pressure is well described by this modified form of the Eyring equation. The need for two processes in parallel was indicated by the curvature of the graphs of yield stress against strain rate. The inclusion of terms to model the effect of pressure on each barrier height implies a non-linear dependence of yield stress on pressure if a sufficiently large range of temperatures and strain rates is considered. In particular it implies an increase of pressure dependence of yield stress when moving from low pressures and strain rates and high temperatures to high pressures and strain rates and low temperatures. The increase in slope occurs under the conditions where the second process makes a significant contribution to the yield stress. The yield data presented here show this effect which has not been previously recognized, although Pampillo and Davis [14] reported a reduction with increasing pressure in the pressure activation volume of the flow stress for ultra-high molecular weight polyethylene tested in tension.

The Erying parameters listed in Table II are comparable with those reported for other isotropic amorphous and crystalline polymers [15] and are also similar to those obtained by Pamillo and Davis [14] and Wu and Turner [16] for the flow stress of ultra-high molecular weight polyethylene. The stress and pressure activation volumes for the first flow process, which contributed to the yield stress over the whole range of test conditions used in these experiments, were considerably larger than those for the second flow process, which contributed a significant amount only at high pressures, high strain rates and low temperatures. Although the physical significance of the activation volumes is not clear, the results obtained here for the two flow processes suggest that the yield mechanism associated with the second flow process which contributed to the yield stress at high pressures, high strain rates or low temperatures was more localized than that associated with the first flow process which contributed to the yield stress over the whole range of test conditions.

5. Conclusions

(1) It was found that a ductile–brittle transition could be induced in even comparatively tough grades of polyethylene by the application of high hydrostatic pressure. In Rigidex 50 this transition arises in a conventional way because of the greater strain-rate and pressure-dependence of the yield stress compared with the fracture stress.

(2) At low strain rates the strain-rate dependence of the yield stress decreased considerably and a second type of ductile–brittle transition was observed as the yield stress once more exceeded the fracture stress. This type of behaviour where a polymer becomes increasingly brittle with decreasing strain rate has not been seen before.

(3) The fracture stresses of the three grades of polymer, where observed, were similar. Large differences in the toughness of these materials must, therefore, be attributed to differences in the yield behaviour.

(4) The yield behaviour of polyethylene can be described by two Eyring processes operating in parallel, both processes being pressure-dependent. With this simple model the effect of temperature, strain rate and pressure observed here are well described.

Acknowledgements

This work was conducted under a grant from the Polymer Engineering Directorate, S.R.C. The authors wish to thank Dr D. Sims, PERME, Waltham Abbey, for kindly moulding the Rigidex 50 and Rigidex 006-60 samples and B.P. Chemicals, Barry, for supplying the polymers used in this work.

References

1. J. B. HOWARD, in "Engineering Design for Plastics", edited by E. Baer (Van Nostrand, New York, 1964) Chap. 11.
2. S. RABINOWITZ, I. M. WARD and J. S. C. PARRY, *J. Mater. Sci.* 5 (1970) 29.
3. S. H. JOSEPH and R. A. DUCKETT, *Polymer* 19 (1978) 837.
4. A. NADAI, "Theory of Flow and Fracture of Solids", 2nd edn. (McGraw-Hill, New York, 1950) p. 347.

5. A. W. CHRISTIANSEN, E. BAER and S. V. RADCLIFFE, *Phil. Mag.* **24** (1971) 451.
6. D. R. MEARS, K. D. PAE and J. A. SAUER, *J. Appl. Phys.* **40** (1969) 4229.
7. J. S. TRENT, A. Y. MOET, M. J. MILES and E. BAER, *Polymer Eng. Sci.* **18** (1978) 1235.
8. ASTM D2552, Annual Book of ASTM Standards, Part 36, 1980.
9. H. EYRING, *J. Chem. Phys.* **4** (1936) 283.
10. I. M. WARD, *J. Mater. Sci.* **6** (1971) 1397.
11. J. A. ROETLING, *Polymer* **6** (1965) 311.
12. C. BAUWENS-CROWET, J. C. BAUWENS and G. HOMES, *J. Polymer Sci. A2* **7** (1969) 735.
13. R. A. DUCKETT, S. RABINOWITZ and I. M. WARD, *J. Mater. Sci.* **5** (1970) 909.
14. C. A. PAMPILLO and L. A. DAVIS, *J. Appl. Phys.* **43** (1972) 4277.
15. R. N. HAWARD and G. THACKRAY, *Proc. Roy. Soc.* **A302** (1968) 453.
16. W. WU and A. P. L. TURNER, *J. Polymer Sci. Polymer Phys.* **13** (1975) 19.

Received 20 November and accepted 12 December 1980.